

Acta Diabetol (2012) 49:277–289  
DOI 10.1007/s00592-011-0314-9

ORIGINAL ARTICLE

# Molecular mechanisms of muscarinic acetylcholine receptor–stimulated increase in cytosolic free $\text{Ca}^{2+}$ concentration and ERK1/2 activation in the MIN6 pancreatic $\beta$ -cell line

Joanne L. Selway · Claire E. Moore ·  
Rajendra Mistry · R. A. John Challiss ·  
Terence P. Herbert

Received: 4 May 2011 / Accepted: 17 July 2011 / Published online: 11 August 2011  
© The Author(s) 2011. This article is published with open access at [Springerlink.com](http://Springerlink.com)

**Abstract** Muscarinic acetylcholine receptor (mAChR) activation of pancreatic  $\beta$ -cells elevates intracellular  $\text{Ca}^{2+}$  and potentiates glucose-stimulated insulin secretion. In addition, it activates a number of signaling molecules, including ERK1/2, whose activation has been shown to play an important role in regulating pancreatic  $\beta$ -cell function and mass. The aim of this work was to determine how mAChR activation elevates intracellular  $\text{Ca}^{2+}$  concentration ( $[\text{Ca}^{2+}]_i$ ) and activates ERK1/2 in the pancreatic  $\beta$ -cell line MIN6. We demonstrate that agonist-stimulated ERK1/2 activation is dependent on the activation of phospholipase C and an elevation in  $[\text{Ca}^{2+}]_i$ , but is independent of the activation of diacylglycerol-dependent protein kinase C isoenzymes. Using a pharmacological approach, we provide evidence that agonist-induced increases in  $[\text{Ca}^{2+}]_i$  and ERK activity require (1)  $\text{IP}_3$  receptor-mediated mobilization of  $\text{Ca}^{2+}$  from the endoplasmic reticulum, (2) influx of extracellular  $\text{Ca}^{2+}$  through store-operated channels, (3) closure of  $\text{K}_{\text{ATP}}$  channels, and (4)  $\text{Ca}^{2+}$  entry via L-type voltage-operated  $\text{Ca}^{2+}$  channels. Moreover, this  $\text{Ca}^{2+}$ -dependent activation of ERK is mediated via both Ras-dependent and Ras-independent mechanisms. In summary, this study provides important insights into the multifactorial signaling mechanisms linking mAChR activation to increases in  $[\text{Ca}^{2+}]_i$  and ERK activity.

**Keywords** Muscarinic acetylcholine receptor · Extracellular signal-regulated kinase · Acetylcholine · Carbachol · Calcium ·  $\beta$ -cell · Islet

## Introduction

Acetylcholine (ACh) is released by intra-pancreatic vagal nerve endings and activates muscarinic acetylcholine receptors (mAChRs) on pancreatic  $\beta$ -cells during both the pre-absorptive (cephalic phase) and absorptive phases of nutrient intake [1–3]. mAChR activation in the pre-absorptive and absorptive phase potentiates subsequent insulin secretion [1, 2], and these different phases can be modulated independently of each other in both the diabetic and non-diabetic state [4]. Although multiple mAChR subtypes have been reported to be expressed in  $\beta$ -cells (i.e.,  $\text{M}_1$ ,  $\text{M}_3$ , and  $\text{M}_4$ ) [3, 5–8], selective  $\text{M}_3$  mAChR knockout in mice has provided evidence that this receptor subtype is primarily responsible for cholinergic actions in  $\beta$ -cells [3, 9].

The  $\text{M}_3$  mAChR preferentially couples to the  $\text{G}\alpha_{\text{q}/11}$ -phospholipase C $\beta$  (PLC $\beta$ ) signaling pathway. Activation of PLC $\beta$  generates inositol 1,4,5-trisphosphate ( $\text{IP}_3$ ) and diacylglycerol (DAG) through hydrolysis of phosphatidylinositol 4,5-bisphosphate ( $\text{PIP}_2$ ) [10].  $\text{IP}_3$  activates  $\text{IP}_3$  receptors expressed on the endoplasmic reticulum (ER), resulting in the release of  $\text{Ca}^{2+}$  from the ER and an increase in cytoplasmic  $\text{Ca}^{2+}$  concentration ( $[\text{Ca}^{2+}]_i$ ). DAG is required for the activation of DAG-dependent kinases, including both conventional and novel isoenzyme subfamilies of PKC.

Stimulation of mAChRs in a variety of excitable and non-excitable cells has been shown to activate multiple signaling pathways, including the extracellular signal-regulated kinases, ERK1/2. For example, in the neuroblastoma cell line SK-N-BE2(C),  $\text{M}_3$  mAChR activation stimulates ERK1/2 phosphorylation via a PKC $\epsilon$ -, Ras-, Raf- and MEK-dependent mechanism that is independent of  $[\text{Ca}^{2+}]_i$  [11, 12]. In contrast, the activation of ERK1/2 by  $\text{M}_3$  mAChR activation in human glial cells is dependent on

J. L. Selway · C. E. Moore · R. Mistry ·  
R. A. John Challiss · T. P. Herbert (✉)  
Department of Cell Physiology and Pharmacology,  
University of Leicester, Henry Wellcome Building,  
Leicester LE1 9HN, UK  
e-mail: [tph4@le.ac.uk](mailto:tph4@le.ac.uk)

Ca<sup>2+</sup> mobilization [13]. In rat islets of Langerhans, carbachol (carbamylcholine, a stable acetylcholine analog) stimulates ERK1/2 phosphorylation [14], and ERK1/2 activation has been reported to stimulate  $\beta$ -cell proliferation and gene transcription, and to influence cell survival and insulin secretion [15–18]. However, the signaling pathway connecting mAChR to ERK1/2 activation in  $\beta$ -cells is poorly understood. Therefore, the principal aim of this study was to determine the signaling mechanism(s) linking the mAChR to ERK1/2 activation in  $\beta$ -cells.

## Materials and methods

### Chemicals

Nifedipine and diazoxide were purchased from Calbiochem. All other chemicals (unless stated) were obtained from Sigma.

### Cell culture

MIN6 cells were used between passages 25 and 40 at ~80% confluence and grown as described previously [19].

### Cell treatments

Prior to treatment, the medium was removed and cells washed twice with HEPES-balanced Krebs–Ringer bicarbonate (KRB) buffer (115 mM NaCl, 5 mM KCl, 10 mM NaHCO<sub>3</sub>, 2.5 mM MgCl<sub>2</sub>, 2.5 mM CaCl<sub>2</sub>, 20 mM HEPES, pH 7.4). The cells were then incubated for 1 h at 37°C in KRB buffer prior to treatments for the times indicated in the figure legends. All inhibitors were added 30 min prior to treatments. All treatments were stopped by the addition of ice-cold lysis buffer (1% Triton-X100, 10 mM  $\beta$ -glycerophosphate, 50 mM Tris–HCl, pH 7.5, 1 mM EDTA, 1 mM EGTA, 1 mM sodium orthovanadate, 1 mM benzamide HCl, 0.2 mM phenylmethylsulfonyl fluoride, 1  $\mu$ g/mL each of leupeptin and pepstatin, 0.1%  $\beta$ -mercaptoethanol, and 50 mM sodium fluoride). The lysates were then centrifuged at 4°C for 10 min at 16,000 $\times$ g, supernatants kept, and total protein concentrations determined by the Bradford assay (Bio-Rad). The protein lysates were stored at –80°C until further analysis.

### Plasmid DNA constructs and transfections

Transfections of MIN6 cells were carried out only for single-cell imaging studies. The DIER cameleon- [20], eGFP-PH<sub>PLC $\delta$ 1</sub>- [21], and GFP-PKC $\epsilon$ -containing plasmids were provided by Prof. Roger Tsien (University of

California, USA), Prof. Stephen Ferguson (Roberts Research Institute, University of Ontario, Canada) and Prof. Tobias Meyer (Stanford University, USA), respectively. DNA was transfected using LipofectAMINE2000 (Invitrogen) according to the manufacturer's instructions. Transfection efficiency was approximately 10–20% as determined by GFP expression.

### Adenoviral constructs and infection

AdRasN17 was a gift from Prof. B. Kahn and Dr. C. Sutherland [22]. AdEmpty.eGFP has been described previously [23]. MIN6 cells were infected with the viruses for 48 h as previously described [23] prior to performing the experiments. We routinely obtained 90–100% transduction efficiency as assessed by GFP expression.

### SDS–polyacrylamide gel electrophoresis (PAGE) and immunoblotting

SDS–PAGE and Western blotting were performed as previously described [24]. Rabbit anti-phospho-ERK1/2 and anti-ERK2 antibodies were purchased from Cell Signaling Technology. Detection was by horseradish peroxidase-linked anti-rabbit secondary antibodies and enhanced chemiluminescence (Cheshire Biosciences).

### Single-cell confocal Ca<sup>2+</sup> imaging

For Ca<sup>2+</sup> imaging, MIN6 cells were loaded for 30 min at 20°C with 2  $\mu$ M of Fluo-4-AM prepared in dye loading buffer (KRB supplemented with 1 mg/mL BSA and 0.1% Pluronic F-127). The cells were then washed in KRB and incubated for a further 10 min in KRB to allow de-esterification of the indicator. Measurement of changes in fluorescence, as an indicator of [Ca<sup>2+</sup>]<sub>i</sub>, was observed using a PerkinElmer UltraVIEW confocal microscope. Fluo-4 was excited using the 488-nm laser-line and 485-nm excitation filter, and the emitted fluorescence was captured at wavelengths >520 nm, with images collected at approximately 2-s intervals. Raw fluorescence data were expressed as  $F/F_0$ . Data are reported as the mean SEM from at least three individual experiments.

### Population NOVOstar Ca<sup>2+</sup> imaging

Population-based Ca<sup>2+</sup> fluorescence measurements were taken using a NOVOstar microplate reader (BMG Lab-Technologies, Offenburg, Germany). MIN6 cells were grown on a 96-well plate format, were washed twice with KRB buffer and then loaded and equilibrated with 2  $\mu$ M Fluo-4-AM as described previously. Cells were excited at

488 nm, with emission recorded at 520 nm every 0.5 s. Raw fluorescence data were expressed as  $F/F_0$  (stimulated fluorescence/basal fluorescence). Data are reported as the average SEM from at least three individual experiments.

### Single-cell confocal GFP imaging

Confocal imaging was performed using an Olympus *FV300* scanning confocal microscope. Real-time images were taken every second, and cells containing eGFP were excited at 488 nm and emissions collected at 505–560 nm. Application of agonists was via bath addition. Cytosolic and membrane regions of interest were selected and average pixel intensity in that region was plotted against time. Changes in fluorescence intensity were analyzed using Fluoview Tiempo software (version 4.3). Fluorescent intensity at a given time was divided by the initial fluorescence within each region of interest and expressed as  $F/F_0$  SEM.

### FRET imaging

ER luminal  $\text{Ca}^{2+}$  was imaged using the ER-localized FRET-based D1ER cameleon [20]. Application of agonists occurred via bath addition. Images were captured with the 20 $\times$  objective of a Zeiss axiovert 200 M epifluorescence microscope with a CCD camera controlled by Metafluor software. Emission ratio imaging of the cameleon was accomplished using a 436DF20 excitation filter, 450-nm dichroic mirror, and two emission filters (475/40 for enhanced CFP and 535/25 for citrine) controlled by a Lambda 10-2 filter changer. Exposure times were typically 100–1,000 ms, and images were collected every 8–20 s.

### Measurement of [ $^3\text{H}$ ]IP $_x$

For the determination of  $^3\text{H}$ -labeled inositol mono-, bis-, and trisphosphates ([ $^3\text{H}$ ]IP $_x$ ), MIN6 cells were pre-labeled with 2.5  $\mu\text{Ci}/\text{mL}$  *myo*-[ $^3\text{H}$ ]inositol (86 Ci/mmol) for 48 h in 24-well multidishes. Medium was then removed, and the cell monolayers washed and incubated for 30 min in 1 mL of KRB in the absence or presence of 10 mM LiCl (see “Results” section). Carbachol was added as indicated and incubations terminated by rapid aspiration and addition of ice-cold 0.5 M trichloroacetic acid. Samples were neutralized as described previously and the neutral extract applied to Dowex (AG1-X8) formate columns, which was then washed with 20 mL of water and 10 mL of 25 mM ammonium formate. The [ $^3\text{H}$ ]IP $_x$  fraction was eluted with 10 mL of 1 M ammonium formate/0.1 M formic acid and quantified by liquid scintillation spectrometry.

### Measurement of [ $^3\text{H}$ ]phosphoinositides

[ $^3\text{H}$ ]Glycerophosphoinositolphosphates (GroPI, GroPI(4)P and GroPI(4,5)P $_2$ ), as indices of PI, PI(4)P, and PI(4,5)P $_2$ , were prepared from cell monolayers based on previously described methods [25]. After removal of the acidified aqueous phase for the determination of [ $^3\text{H}$ ]IP $_x$  as described above, lipids were extracted into 0.94 mL of acidified chloroform/methanol (40:80:1 v/v, 10 M HCl). Chloroform (0.31 mL) and 0.1 M HCl (0.56 mL) were then added to induce phase partition. A sample of the lower phase (450  $\mu\text{L}$ ) was removed and dried in a stream of  $\text{N}_2$ . Dried samples were dissolved in 1 mL of chloroform and 0.2 mL of methanol and hydrolyzed by the addition of 0.4 mL of 0.5 M NaOH in methanol/water (19:1, v/v). Samples were vortex-mixed at regular intervals during a 20-min incubation at 25°C. Chloroform (1 mL), methanol (0.6 mL), and water (0.6 mL) were then added, and the samples were mixed and centrifuged (3,000  $\times g$ , 10 min). A 1-mL aliquot of the upper phase was neutralized using 1-mL bed volume of Dowex-50 ( $\text{H}^+$  form) columns that were washed with 2  $\times$  2 mL of water. The pooled eluate was brought to pH 7 by the addition of  $\text{NaHCO}_3$  and applied to a Dowex (AG1-X8) formate anion exchange column. The [ $^3\text{H}$ ]GroPI, [ $^3\text{H}$ ]GroPI(4)P, and [ $^3\text{H}$ ]GroPI(4, 5)P $_2$  were then eluted as described elsewhere [25] and quantified by liquid scintillation spectrometry.

### Statistical analysis

Statistical differences between multiple groups were analyzed via either single-factor or two-way analysis of variance (ANOVA), followed by post hoc analysis as described in figure legends. A statistical test was only carried out when the experiments have at least  $n = 3$ . Statistical analyses were performed in GraphPad Prism, and significance was only confirmed when  $P < 0.05$  (\* $P < 0.05$ ; \*\* $P < 0.01$ ; \*\*\* $P < 0.001$ ).

## Results

### Characterization of carbachol-stimulated ERK1/2 phosphorylation in the pancreatic $\beta$ -cell line MIN6

Carbachol addition caused a rapid, transient increase in the phosphorylation of ERK1/2 (peaking at 2 min and rapidly returning to basal levels within 10 min; Fig. 1a). The carbachol-stimulated phosphorylation of ERK1/2 at 2 min was concentration dependent, yielding an  $\text{EC}_{50}$  value of approx. 7  $\mu\text{M}$  (Fig. 1b). Carbachol addition also stimulated a rapid, concentration-dependent increase in  $[\text{Ca}^{2+}]_i$  ( $\text{EC}_{50}$  value approx. 0.9  $\mu\text{M}$ ) (Fig. 1c). To confirm that carbachol

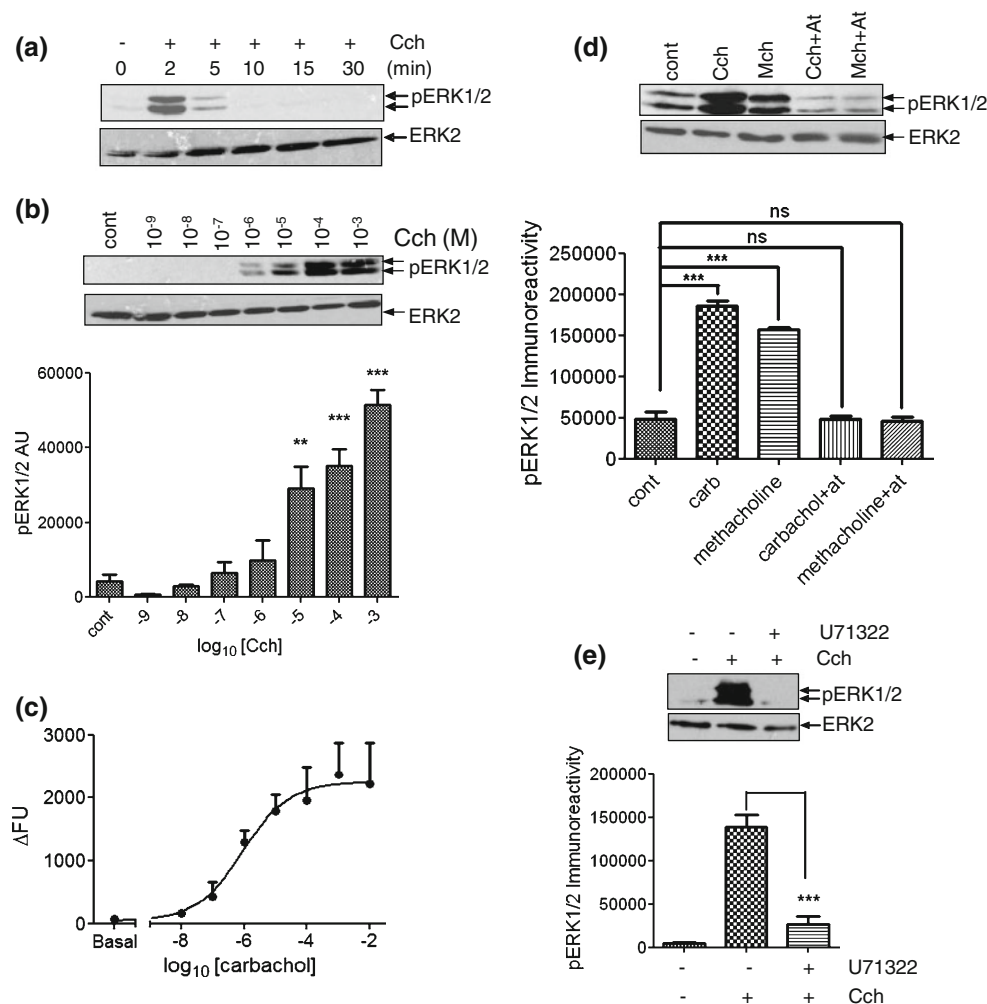


**Fig. 1** Characterization of carbachol-stimulated increase in  $[Ca^{2+}]_i$  and ERK1/2 activation. MIN6 cells pre-incubated for 1 h with KRBrminus-glucose; **a** Carbachol (1 mM) for the times indicated; **b** carbachol at the concentrations indicated for 2 min. Proteins were separated by SDS-PAGE and detected by Western blotting using anti-phospho-ERK1/2 and anti-ERK2 antibodies. Data shown in lower panel are means + SEM ( $n = 3$ ).  $**P < 0.01$ ,  $***P < 0.001$ ; one-way ANOVA followed by Dunnett's range test comparing to no carbachol addition. **c** Concentration–response curve for carbachol-stimulated increases in  $[Ca^{2+}]_i$  determined in cell populations using a NOVOstar plate reader. Data represent means SEM ( $n = 3$ ) of the peak change in fluorescence ( $\Delta FU$ ) correlating with peak increases in  $[Ca^{2+}]_i$ . **d** Where indicated, cells were incubated with atropine (At,

10  $\mu M$ ) for 30 min prior to treatment with carbachol (Cch, 1 mM) or methacholine (Mch, 1 mM) for 2 min. Proteins were separated by SDS-PAGE and detected by Western blotting using anti-phospho-ERK1/2 and anti-ERK2 antibodies. Data shown in lower panel are means SEM ( $n = 3$ ); *ns* no significance,  $***P < 0.001$  by Dunnett's range test following one-way ANOVA comparing to no carbachol addition. **e** MIN6 cells were pre-treated with U71322 (1  $\mu M$ ) for 30 min prior to treatment with carbachol (1 mM, 2 min). Proteins were separated by SDS-PAGE and detected by Western blotting using anti-phospho-ERK1/2 and anti-ERK2 antibodies. Lower panel are means SEM ( $n = 3$ ). Data were analyzed by a Student's 2-tailed  $t$  test;  $***P < 0.001$ . All immunoblots shown are representative of three independent experiments

was mediating these actions via mAChR activation, MIN6 cells were treated with carbachol, or the mAChR-selective agonist methacholine, in the absence and presence of the mAChR antagonist atropine. Both the carbachol- and methacholine-stimulated phosphorylations of ERK1/2 were completely inhibited in the presence of atropine (Fig. 1d).

To examine the role of PLC in carbachol-stimulated ERK1/2 phosphorylation, MIN6 cells were treated with carbachol in the absence or presence of the PLC inhibitor

U71322. U71322 completely prevented carbachol-stimulated ERK1/2 activation (Fig. 1e).

Carbachol-stimulated ERK1/2 activation is MEK dependent and occurs via both Ras-dependent and Ras-independent mechanisms

To investigate the role of Ras in carbachol-stimulated ERK1/2 phosphorylation, MIN6 cells were infected with a

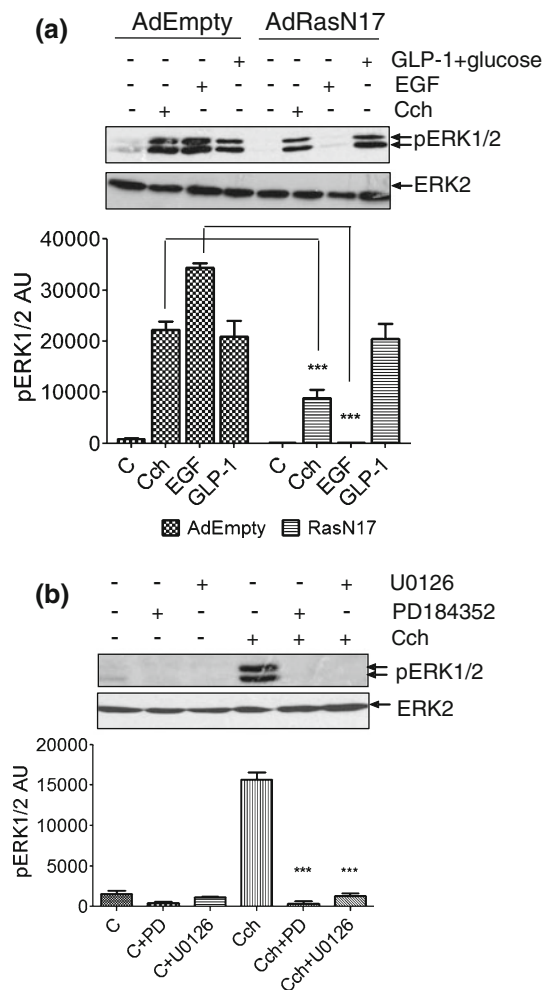


**Fig. 2** Role of Ras and MEK in carbachol-stimulated ERK1/2 activation. **a** MIN6 cells were infected with a control adenovirus (AdEmpty.eGFP) or with an adenovirus engineered for expression of RasN17 (AdRasN17). After 48 h, cells were pre-incubated for 1 h with KRB-minus-glucose before treatment with carbachol (1 mM, 2 min), EGF (20 ng/ml, 5 min) or GLP-1 (10 nM) plus 16.7 mM glucose for 10 min. **b** MIN6 cells were pre-incubated for 1 h in KRB and where indicated PD098059 (PD, 1  $\mu$ M) or U0126 (20  $\mu$ M) was added for the last 30 min before addition of carbachol (1 mM, 2 min). Proteins were separated by SDS-PAGE and detected by Western blotting using anti-phospho-ERK1/2 and anti-ERK2 antibodies. Below each representative blot is a graph showing densitometric quantification of ERK1/2 phosphorylation. Data are presented as means SEM ( $n = 3$ ); \*\*\* $P < 0.001$  by Dunnett's range test following one-way ANOVA compared to the carbachol response

recombinant adenovirus expressing dominant-negative Ras (RasN17), and 48 h post-infection, cells were treated with carbachol, EGF (which activate ERK1/2 in a Ras-dependent manner) or GLP1 (which activates ERK1/2 in a Ras-independent manner) [23]. As expected, RasN17 completely inhibited EGF-stimulated ERK1/2 phosphorylation and was without effect on the GLP1-stimulated response (Fig. 2a). mAChR-mediated phosphorylation of ERK1/2 was only partially inhibited, indicating that

carbachol can activate ERK1/2 by both Ras-dependent and Ras-independent mechanisms (Fig. 2a). To determine whether carbachol-stimulated ERK1/2 phosphorylation is mediated by MEK, MIN6 cells were treated with carbachol in the absence or presence of two structurally distinct MEK inhibitors, PD184352 and U0126. Either inhibitor completely abolished carbachol-stimulated ERK1/2 phosphorylation (Fig. 2b).

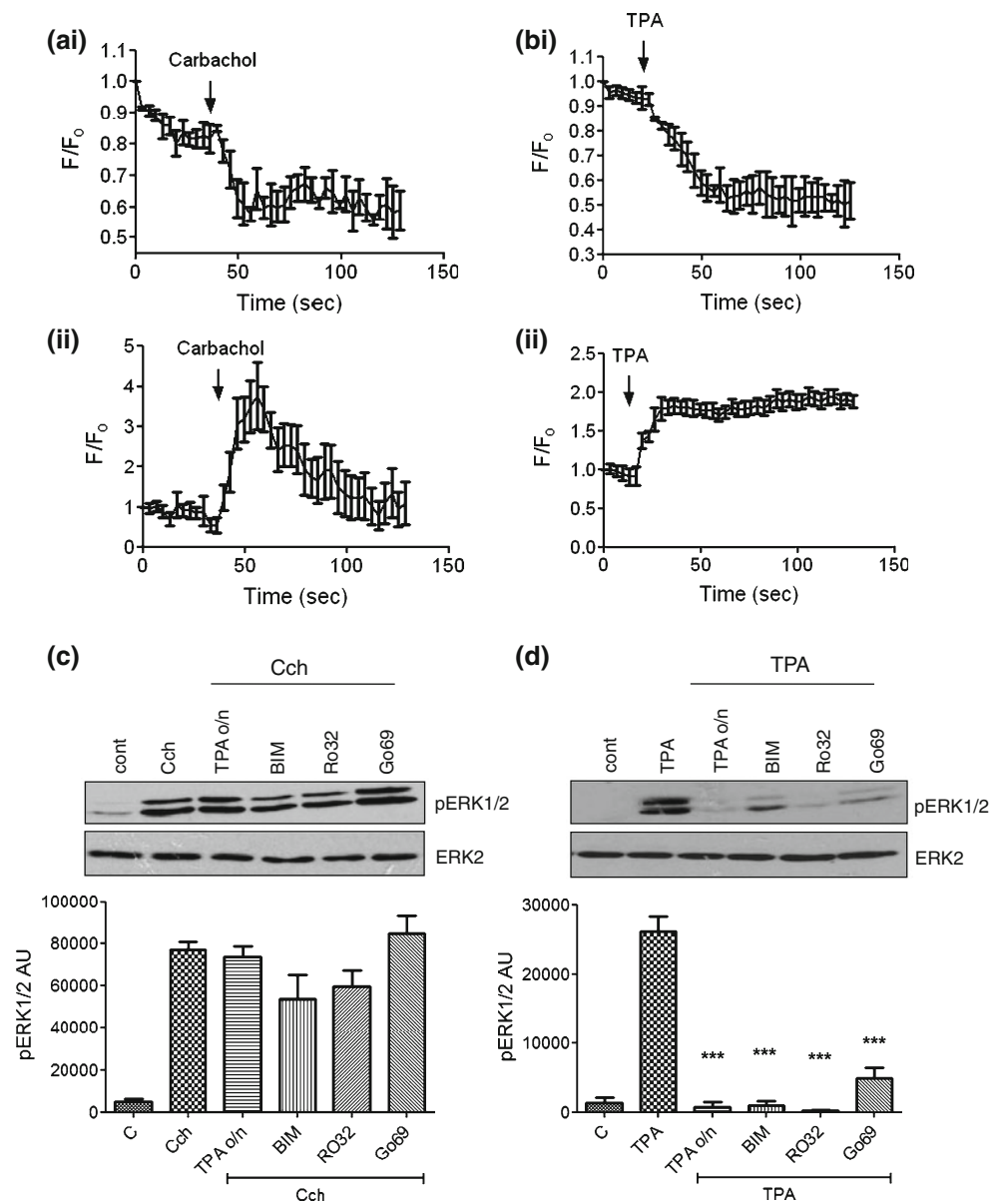
Carbachol-stimulated ERK1/2 phosphorylation is independent of the activation of both conventional and novel isoenzymes of PKC

Activation of PLC $\beta$  by the M<sub>3</sub> mAChR results in the hydrolysis of PIP<sub>2</sub> to generate IP<sub>3</sub> and DAG [10, 26]. DAG is required for the activation of DAG-dependent kinases, including conventional and novel PKC isoenzymes [27], which have been implicated in mAChR activation of ERK1/2 [11, 12]. To confirm that carbachol activates the PLC-DAG-PKC pathway in  $\beta$ -cells, MIN6 cells were transfected with GFP-tagged PKC $\epsilon$  (GFP-PKC $\epsilon$ ). Translocation of this biosensor to the plasma membrane is indicative of an increase in the concentration of DAG and the activation of PKC. Both carbachol (Fig. 3a) and 12-*o*-tetradecanoylphorbol-13-acetate (TPA, a DAG-mimetic, used as a positive control; Fig. 3b) treatment resulted in translocations of GFP-PKC $\epsilon$  from the cytosol to the plasma membrane. To investigate the role of DAG-dependent PKCs in carbachol-stimulated ERK1/2 activation, MIN6 cells were treated with carbachol or TPA in the absence or presence of the PKC inhibitors, bisindolylmaleimide I (BIM I), Ro 32-0432 and Gö6976, which inhibit both conventional and novel PKCs [28–30]. In addition, MIN6 cells were stimulated with TPA overnight to down-regulate the expression of all DAG-dependent PKCs [24, 27] before treatment with carbachol or TPA. None of the PKC inhibitors, or chronic TPA pre-treatment, significantly inhibited carbachol-induced ERK1/2 activation (Fig. 3c), whereas each manipulation substantially inhibited acute TPA-stimulated ERK1/2 activation (Fig. 3d).

Increases in [Ca<sup>2+</sup>]<sub>i</sub> are essential for carbachol-stimulated ERK1/2 phosphorylation

Carbachol stimulated concentration-dependent increases in [Ca<sup>2+</sup>]<sub>i</sub> that paralleled ERK1/2 activation (Fig. 1b, c). To determine whether this increase in [Ca<sup>2+</sup>]<sub>i</sub> was essential for ERK1/2 activation, MIN6 cells were loaded with the Ca<sup>2+</sup> chelator BAPTA-AM prior to carbachol addition. BAPTA-AM substantially attenuated carbachol-induced ERK1/2 activation (Fig. 4a) and abolished the agonist-stimulated change in [Ca<sup>2+</sup>]<sub>i</sub> (Fig. 4b). Incubation of MIN6 cells in EGTA-buffered KRB (resulting in a [Ca<sup>2+</sup>]<sub>i</sub> of approx. 100

**Fig. 3** PKC requirement for carbachol-mediated ERK1/2 activation. MIN6 cells, transfected to express eGFP-tagged PKC $\epsilon$ , were pre-incubated for 1 h in KRB-minus-glucose prior to treatment with **a** carbachol (1 mM) or **b** TPA (1  $\mu$ M). Fluorescence intensity in the (i) cytoplasm or (ii) at the membrane was monitored by fluorescence confocal microscopy. Changes in fluorescence intensity were expressed relative to initial fluorescence ( $F/F_0$ ). **c**, **d** MIN6 cells pre-treated in the absence or presence of TPA (1  $\mu$ M) for 16 h (TPA o/n) were pre-incubated for 1 h in KRB-minus-glucose prior to treatment with **c** carbachol (1 mM, 2 min) or **d** TPA (1  $\mu$ M, 60 min) in the absence or presence of bisindolylmaleimide I (BIM, 1  $\mu$ M), Ro 32-0432 (Ro32, 1  $\mu$ M), or Gö6976 (Go69, 1  $\mu$ M). Proteins were separated by SDS-PAGE and detected by Western blotting using anti-phospho-ERK1/2 and anti-ERK2 antibodies. Representative blots are shown *above* with mean data densitometry *below* in panels **c** and **d**. Data are shown as means  $\pm$  SEM ( $n = 3$ ); \*\*\* $P < 0.001$  by Dunnett's range test following one-way ANOVA compared to carbachol (panel **c**) or TPA (panel **d**)



nM abolishing the transmembrane  $[Ca^{2+}]_i$  gradient) inhibited both carbachol-stimulated ERK1/2 activation (Fig. 4c) and the increase in  $[Ca^{2+}]_i$  (Fig. 4d). Therefore, carbachol-stimulated ERK1/2 activation is dependent on an increase in  $[Ca^{2+}]_i$ , which is primarily dependent on  $Ca^{2+}$  influx.

Investigating the mechanism of carbachol-induced increases in  $[Ca^{2+}]_i$  and ERK1/2 phosphorylation

To investigate how carbachol elicits an increase in  $[Ca^{2+}]_i$  and to gain an insight into how this may lead to ERK1/2 activation, MIN6 cells were pre-incubated with nifedipine (10  $\mu$ M; an L-type voltage-operated  $Ca^{2+}$  channel (VOC) blocker), diazoxide (250  $\mu$ M; a  $K_{ATP}$  channel activator), 2-APB (10  $\mu$ M; a store-operated  $Ca^{2+}$  channel (SOC) and  $IP_3$  receptor inhibitor), xestospongin C (10  $\mu$ M; an  $IP_3$

receptor antagonist), or thapsigargin (1  $\mu$ M; a SERCA pump inhibitor, which leads to ER  $Ca^{2+}$  store depletion) before carbachol addition.

Pre-treatment of MIN6 cells with nifedipine or diazoxide effectively abolished carbachol-induced ERK1/2 activation and peak  $[Ca^{2+}]_i$  (Fig. 5a, b). These data indicate that the activation of the L-type VOCs is required for carbachol-induced  $Ca^{2+}$  influx and ERK1/2 activation, while the diazoxide effect suggests a potential involvement of  $K_{ATP}$ . The  $IP_3$  receptor antagonists, xestospongin C and 2-APB, also significantly attenuated carbachol-stimulated ERK1/2 activation and peak  $[Ca^{2+}]_i$ . However, xestospongin C was unable to block completely increases in  $[Ca^{2+}]_i$  (Fig. 5a, b). To determine the effectiveness of xestospongin C and 2-APB in inhibiting  $IP_3$  receptor-mediated  $Ca^{2+}$ -release, MIN6 cells were pre-incubated

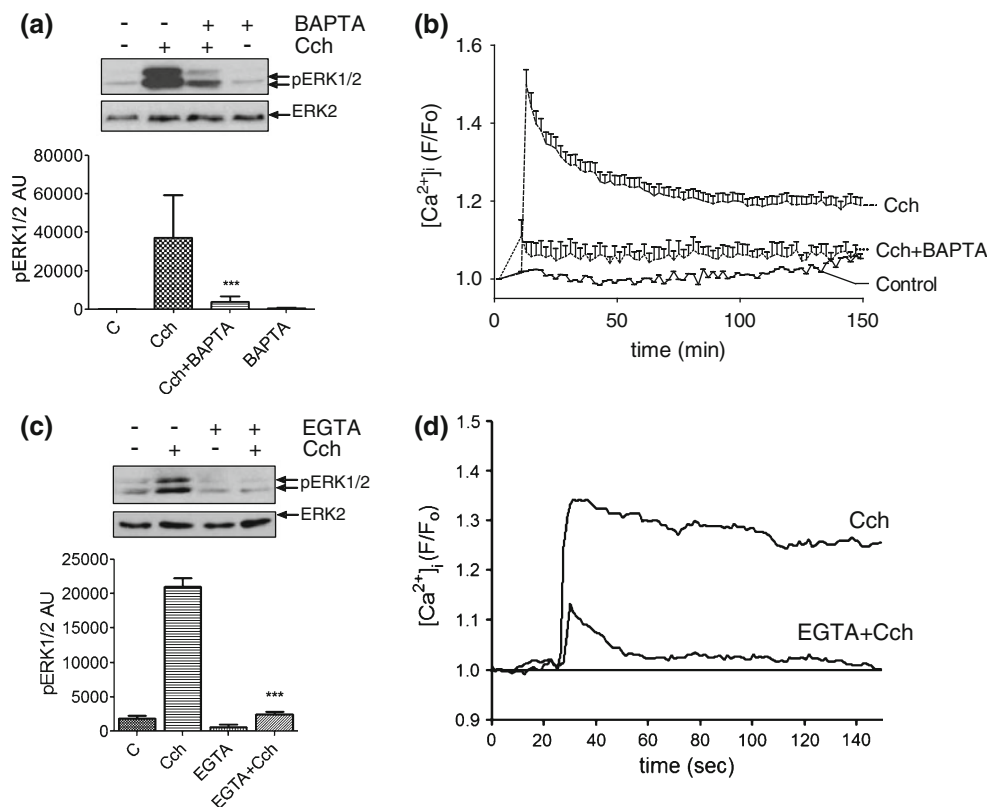


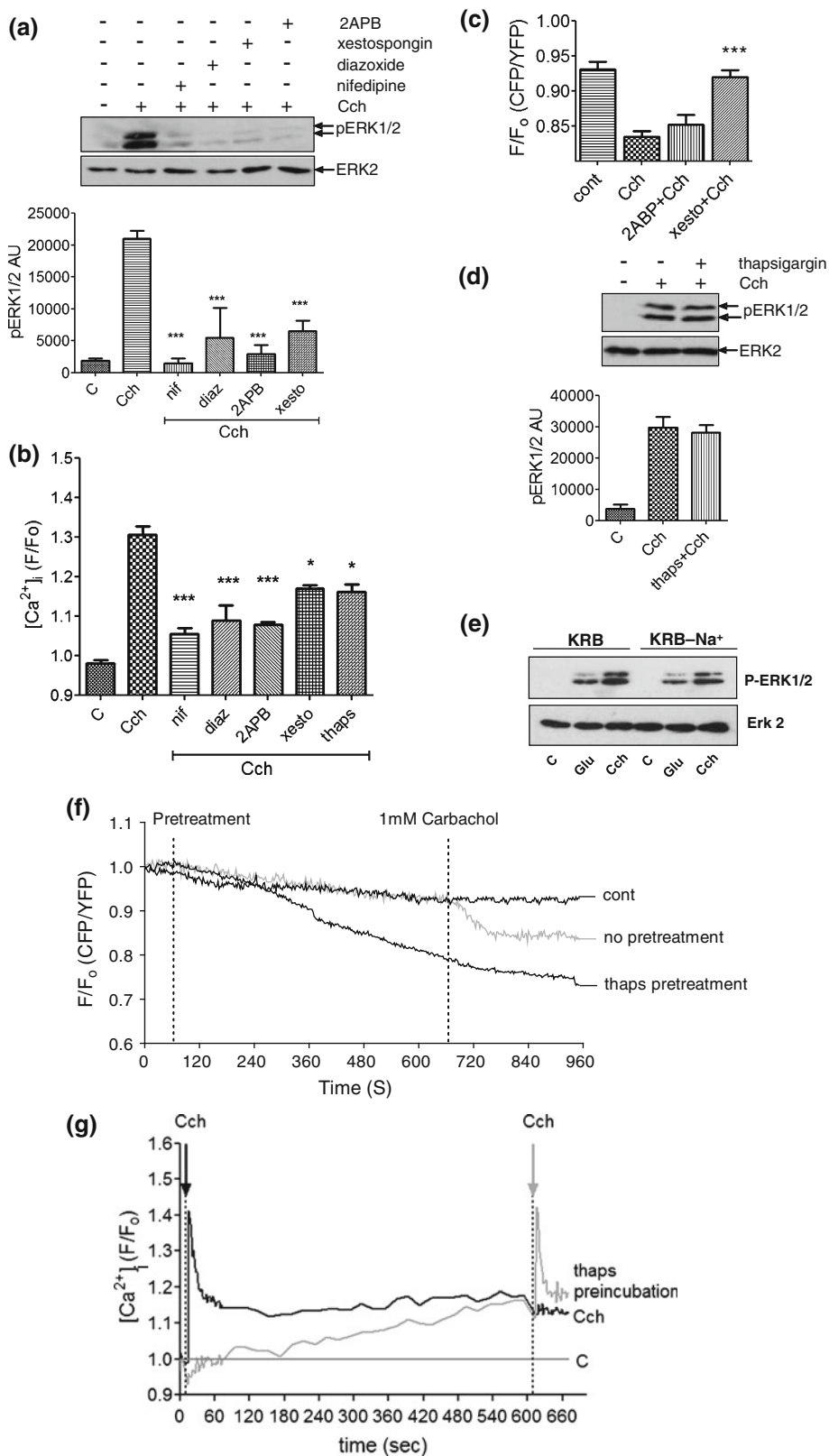
**Fig. 4** Ca<sup>2+</sup> influx across the plasma membrane is required for carbachol-stimulated ERK1/2 activation. **a** MIN6 cells were pre-incubated for 30 min in KRB-minus-glucose and, where indicated, loaded with BAPTA-AM (100 μM, BAPTA) for 30 min. Cells were then treated with carbachol (1 mM, 2 min). Proteins were separated by SDS-PAGE and detected by Western blotting using anti-phospho-ERK1/2 and anti-ERK2 antibodies. A representative blot is shown above with mean data densitometry below. Data are shown as means SEM (*n* = 3); \*\*\**P* < 0.001 by Dunnett's range test following one-way ANOVA compared to carbachol. **b** Cells were loaded with Fluo-4-AM (2 μM) at the same time as BAPTA-AM and [Ca<sup>2+</sup>]<sub>i</sub> measured using single-cell confocal Ca<sup>2+</sup> imaging following carbachol (1 mM) addition. Data represent means SEM for the increase in [Ca<sup>2+</sup>]<sub>i</sub> levels

(*n* > 30). **c** MIN6 cells were pre-incubated for 30 min in KRB-minus-glucose and, where indicated, incubated in EGTA-buffered KRB for the last 10 min. The Ca<sup>2+</sup> concentration in the KRB was reduced to ≤ 100 nM by EGTA-buffering and confirmed using Fura-2 free acid and standard fluorimetry. Carbachol (1 mM) was added to the KRB for 2 min. Proteins were separated by SDS-PAGE and detected by Western blotting using anti-phospho-ERK1/2 and anti-ERK2 antibodies. A representative blot is shown above with densitometry below. Data are means SEM (*n* > 3); \*\*\**P* < 0.001 by Dunnett's range test following one-way ANOVA compared to carbachol. **d** Changes in [Ca<sup>2+</sup>]<sub>i</sub> were assessed by single-cell confocal Ca<sup>2+</sup> imaging reproducing the experimental conditions used in panel **c**

with these inhibitors and the [Ca<sup>2+</sup>]<sub>ER</sub> within the endoplasmic reticulum lumen ([Ca<sup>2+</sup>]<sub>ER</sub>) measured using the D1ER FRET sensor [20]. Stimulation of MIN6 cells with carbachol caused a decrease in [Ca<sup>2+</sup>]<sub>ER</sub> (Fig. 5c), which was prevented by xestospongine C (Fig. 5c). In contrast, 2-APB had no significant effect on carbachol-induced decreases in [Ca<sup>2+</sup>]<sub>ER</sub> (Fig. 5c), demonstrating that it is not effective in MIN6 cells as an IP<sub>3</sub> receptor antagonist. Therefore, the inhibitory effect of 2-APB on carbachol-induced ERK1/2 activation and Ca<sup>2+</sup> mobilization is likely to be occurring through an action at SOCs, another known target of this inhibitor [31].

Although we have demonstrated that IP<sub>3</sub> receptor antagonism prevents carbachol-induced ERK1/2 activation in MIN6 cells, pre-treatment of MIN6 cells with thapsigargin failed to inhibit carbachol-stimulated ERK1/2

activation (Fig. 5d), yet significantly lowered the peak [Ca<sup>2+</sup>]<sub>i</sub> response (Fig. 5b). To determine whether thapsigargin is emptying ER stores of Ca<sup>2+</sup>, MIN6 cells were pre-incubated with 1 μM thapsigargin for 10 min and [Ca<sup>2+</sup>]<sub>ER</sub> measured (Fig. 5f). This resulted in a decrease in [Ca<sup>2+</sup>]<sub>ER</sub>. Yet, the subsequent application of carbachol did not lead to a further decrease in [Ca<sup>2+</sup>]<sub>ER</sub> (Fig. 5f), indicating that thapsigargin had indeed depleted the ER of Ca<sup>2+</sup>. So why is pre-treatment with thapsigargin unable to inhibit carbachol-stimulated ERK1/2 activation? One explanation for this apparent paradox is that thapsigargin is increasing the [Ca<sup>2+</sup>]<sub>i</sub> sufficiently to compensate for the loss of IP<sub>3</sub>-mediated Ca<sup>2+</sup> efflux from the ER. To investigate this possibility, changes in [Ca<sup>2+</sup>]<sub>i</sub> was measured during the thapsigargin pre-treatment and on subsequent carbachol addition. Indeed, it was shown that thapsigargin



pre-incubation caused a significant increase in  $[Ca^{2+}]_i$  levels over the 10-min period (Fig. 5g), yet carbachol-stimulated increases in  $[Ca^{2+}]_i$  were unaffected. Therefore,

it is possible that the increase in  $[Ca^{2+}]_i$  caused by thapsigargin pre-treatment is sufficient to recapitulate IP<sub>3</sub> receptor-mediated  $[Ca^{2+}]_{ER}$  release evoked on carbachol



◀ **Fig. 5** Multiple  $\text{Ca}^{2+}$  sources are required for carbachol-stimulated ERK1/2 activation. **a** MIN6 cells were pre-incubated for 1 h with KRB-minus-glucose in the absence or presence of 2APB (10  $\mu\text{M}$ ) for 30 min, or nifedipine (10  $\mu\text{M}$ ), xestospongine C (10  $\mu\text{M}$ ) or diazoxide (250  $\mu\text{M}$ ) for 10 min prior to carbachol (1 mM, 2 min) addition. Proteins were separated by SDS-PAGE and detected by Western blotting using anti-phospho-ERK1/2 and anti-ERK2 antibodies. A representative blot is shown *above* with mean data densitometry *below*. Data are shown as means SEM ( $n = 3$ );  $*P < 0.05$ ;  $***P < 0.001$  by Dunnett's range test following one-way ANOVA compared to carbachol addition. **b**  $[\text{Ca}^{2+}]_i$  was monitored in populations of MIN6 cells pre-treated as in **a** by NOVOstar plate reader. Data are shown as means SEM ( $n = 3$ );  $*P < 0.05$ ;  $***P < 0.001$  by Dunnett's range test following one-way ANOVA compared to carbachol addition. **c** MIN6 cells transfected with the cameleon DIER construct were pre-incubated for 1 h in KRB-minus-glucose. Cells were then incubated in the absence or presence of 2APB (10  $\mu\text{M}$ ) or xestospongine C (10  $\mu\text{M}$ ) for 10 min before the addition of carbachol (Cch, 1 mM). Data shown represent *peak* FRET changes after agonist addition. **d** MIN6 cells were treated as in **a**, but in the absence or presence of thapsigargin (1  $\mu\text{M}$ ) pre-addition for 10 min. A representative blot is shown *above* with mean data densitometry *below*. **e** MIN6 cells were maintained in KRB in which  $\text{Na}^+$  was replaced by methylglucamine for 15 min before stimulation with either glucose (20 mM) or carbachol (1 mM). Data are shown as means SEM ( $n = 3$ );  $*P < 0.05$ ;  $***P < 0.001$  by Dunnett's range test following one-way ANOVA compared to carbachol. **f** MIN6 cells transfected with cameleon DIER were pre-incubated for 1 h in KRB-minus-glucose prior to recording. All recordings show 1 min of basal KRB perfusion before either no pre-treatment or thapsigargin (1  $\mu\text{M}$ ) addition for 10 min followed by the addition of carbachol (1 mM) for 5 min. Data shown represent mean changes in FRET for  $n \geq 30$  cells. **g** MIN6 cells were pre-incubated in KRB-minus-glucose and then treated with carbachol (1 mM, *black line*) or thapsigargin (1  $\mu\text{M}$ , *gray line*) for 10 min followed by the addition of carbachol (1 mM). Fluorescence was measured as an indicator of  $[\text{Ca}^{2+}]_i$  by NOVOstar plate reader for 10 s before initial Cch/thapsigargin pre-treatments

treatment and thus explain why thapsigargin treatment has no significant effect on carbachol-stimulated increases in  $[\text{Ca}^{2+}]_i$  or ERK1/2 activation.

It has been reported that ACh depolarizes the  $\beta$ -cell by increasing its membrane permeability to  $\text{Na}^+$  [32]. However, the replacement of extracellular  $\text{Na}^+$  with *N*-methyl-glucamine had no significant effect on carbachol-stimulated ERK activation (Fig. 5e).

Taken together, these data provide evidence that carbachol-evoked increases in intracellular  $\text{Ca}^{2+}$  and ERK1/2 activation are mediated by (1) the release of  $\text{Ca}^{2+}$  from ER stores via  $\text{IP}_3$  receptor activation; (2) the influx of extracellular  $\text{Ca}^{2+}$  through activation of SOCs and; (3) depolarization and activation of L-type VOCs, likely through  $\text{K}_{\text{ATP}}$  channel closure.

Characterization of changes in membrane phosphoinositides in response to  $\text{M}_3$  mAChR stimulation

Changes in the ATP/ADP ratio and phosphatidylinositol 4,5-bisphosphate ( $\text{PIP}_2$ ) concentration are known to

regulate  $\text{K}_{\text{ATP}}$  channel activity in pancreatic  $\beta$ -cells [33–35]. However, the ATP/ADP ratio is unlikely to change on mAChR activation alone in the absence of glucose. Therefore, we hypothesized that carbachol may be stimulating  $\text{K}_{\text{ATP}}$  channel closure through agonist-stimulated decreases in  $\text{PIP}_2$  concentration at the plasma membrane. The membrane association of the PH-domain of  $\text{PLC}\delta 1$  fused to eGFP (eGFP-PH $_{\text{PLC}\delta 1}$ ) has been used as a biosensor to assess inositol 1,4,5-trisphosphate ( $\text{IP}_3$ ) generation and changes in  $\text{PIP}_2$  concentration at the single-cell level [36–41]. Therefore, to indirectly measure changes in  $[\text{IP}_3]$  and/or  $[\text{PIP}_2]$ , MIN6 cells were transfected with eGFP-PH $_{\text{PLC}\delta 1}$  and changes in fluorescence determined in response to carbachol. In unstimulated MIN6 cells, the eGFP-PH $_{\text{PLC}\delta 1}$  is localized at the plasma membrane. On carbachol stimulation, eGFP-PH $_{\text{PLC}\delta 1}$  translocated to the cytosol (Fig. 6a) with a corresponding reduction in fluorescence at the plasma membrane (Fig. 6a), indicative of an increase in  $[\text{IP}_3]$  and/or a reduction in plasma membrane  $[\text{PIP}_2]$ . To extend these observations, we determined biochemically whether carbachol stimulation of MIN6 cells caused changes in phosphatidylinositol (PI), phosphatidylinositol 4-phosphate (PIP), and  $\text{PIP}_2$  concentration at the plasma membrane in [ $^3\text{H}$ ]inositol-labeled MIN6 cells. PIP and  $\text{PIP}_2$  were found to make up only a small proportion (1.7 and 2.3%, respectively) of the total phosphoinositide pool. Stimulation with carbachol for 60 s decreased  $\text{PIP}_2$  to  $85 \pm 2\%$  and PIP to  $73 \pm 3\%$  of their respective initial values. These changes were maintained throughout the time course of agonist stimulation ( $\text{PIP}_2$ ,  $89 \pm 1\%$  and PIP,  $68 \pm 5\%$  of pre-stimulation values at 15 min post-carbachol addition; Fig. 6bii). The greater decrease in PIP compared to  $\text{PIP}_2$  suggests that the latter polyphosphoinositide is relatively protected from agonist-induced changes by greater changes in its immediate precursor.

## Discussion

The present study provides evidence that carbachol, through the activation of a  $\text{G}_q$ -coupled mAChR, results in a transient MEK-dependent phosphorylation of ERK1/2 in the pancreatic  $\beta$ -cell line MIN6. We show that carbachol-induced activation of ERK is independent of both the activation of novel and classical PKCs, but is dependent on an increase in  $[\text{Ca}^{2+}]_i$ . We also show that this increase in  $[\text{Ca}^{2+}]_i$  is likely mediated by both an  $\text{IP}_3$ -dependent efflux of  $\text{Ca}^{2+}$  from the endoplasmic reticulum and the influx of extracellular  $\text{Ca}^{2+}$  through both store-operated (SOC) and L-type voltage-operated (VOC)  $\text{Ca}^{2+}$  channels (see Fig. 7).

mAChR activation in MIN6 cells leads to an  $\text{IP}_3$  receptor-dependent efflux of  $\text{Ca}^{2+}$  from the ER. This is

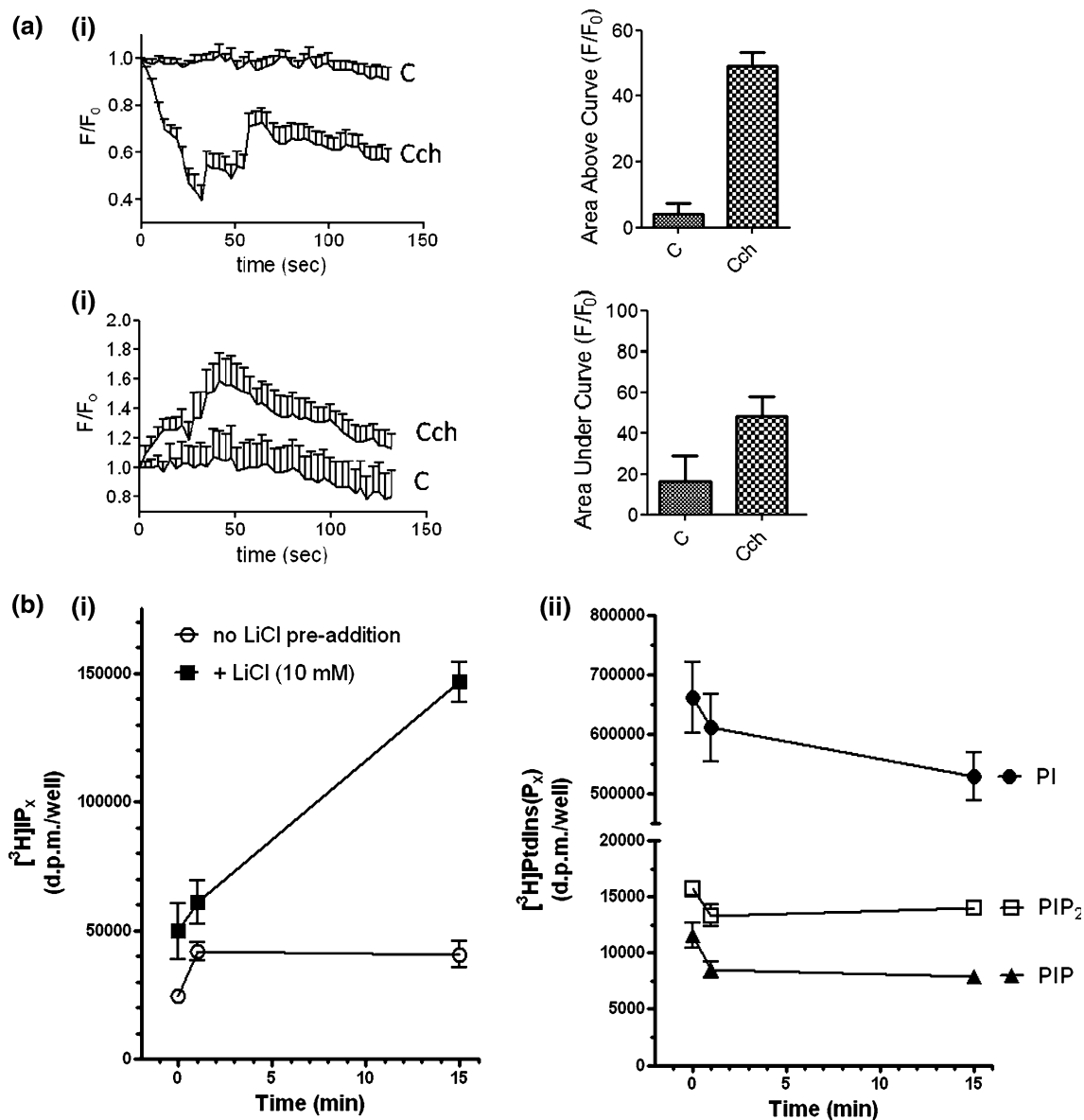


**Fig. 6** Changes in phosphoinositide turnover in MIN6 cells in response to carbachol. **a** MIN6 cells were transfected with a plasmid encoding eGFP-PH<sub>PLC $\delta$ 1</sub>. Cells were then pre-treated for 1 h with KRB-minus-glucose and treated with carbachol (1 mM). Changes in fluorescence intensity at the plasma membrane (*i*) or in the cytoplasm (*ii*) were determined by confocal microscopy. Fluorescence intensity was referenced to the initial fluorescence ( $F/F_0$ ). The area *under* the baseline for membrane fluorescence or *over* the baseline for cytoplasmic fluorescence was calculated and compared between control and carbachol-stimulated cells. Data are presented as means

SEM ( $n > 30$ ). **b** MIN6 cells were incubated with [<sup>3</sup>H]inositol for 48 h. Cells were pre-incubated for 1 h with KRB-minus-glucose and, where indicated, LiCl (10 mM) was added for the final 30 min. Cells were challenged with carbachol (1 mM) for the times indicated and [<sup>3</sup>H]IP<sub>x</sub> and [<sup>3</sup>H]PtdIns(P<sub>x</sub>) fractions recovered and analyzed as described in the “Methods” section. Time-dependent effects of carbachol stimulation on (*i*) [<sup>3</sup>H]IP<sub>x</sub> accumulations in the absence and presence of LiCl and (*ii*) [<sup>3</sup>H]PtdIns, [<sup>3</sup>H]PtdInsP and [<sup>3</sup>H]PtdInsP<sub>2</sub>. Data are shown as means + SEM for 3 independent experiments performed in duplicate

required for, but is not sufficient to cause, the activation of ERK1/2, as carbachol-stimulated ERK1/2 activation also requires the influx of extracellular Ca<sup>2+</sup>. This influx of Ca<sup>2+</sup> is likely via SOCs and L-type VOCs as the increase in [Ca<sup>2+</sup>]<sub>i</sub>, and indeed ERK1/2 phosphorylation, is blocked by either 2-APB (an inhibitor of SOCs, which does not

inhibit IP<sub>3</sub> receptors in this cell type) or nifedipine (an L-type VOC antagonist). As depolarization is a prerequisite for L-type VOC activation and carbachol-stimulated increases in [Ca<sup>2+</sup>]<sub>i</sub> are nifedipine-sensitive, carbachol must induce membrane depolarization. This is likely mediated by multiple mechanisms, including K<sub>ATP</sub> channel

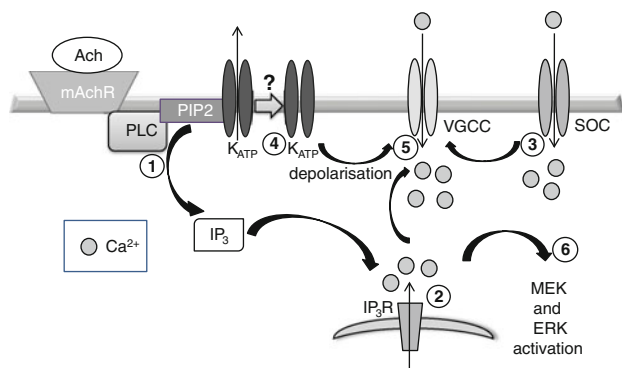


**Fig. 7** Schematic synopsis of the mechanisms of carbachol-stimulated ERK1/2 activation in MIN6 cells. (1) Agonist binding to the mAChR activates PLC resulting in phosphoinositide hydrolysis and the production of IP<sub>3</sub>; (2) activation of IP<sub>3</sub>Rs in the ER increases cytoplasmic [Ca<sup>2+</sup>]<sub>i</sub>; (3) plasma membrane store-operated channels mediate Ca<sup>2+</sup> entry; (4) K<sub>ATP</sub> channels are inactivated; (5) steps 2–4 converge resulting in depolarization and Ca<sup>2+</sup> entry through L-type VGCCs. The increase in [Ca<sup>2+</sup>]<sub>i</sub> results in ERK1/2 activation

closure, Ca<sup>2+</sup> release from the ER via IP<sub>3</sub> receptors, and Ca<sup>2+</sup> influx via SOCs, as both carbachol-stimulated ERK1/2 phosphorylation and increased [Ca<sup>2+</sup>]<sub>i</sub> are significantly inhibited by diazoxide, 2APB and xestospongin C. These results are in general agreement with, and extend, previous observations showing that mAChR activation, in the absence of glucose, stimulates increases in [Ca<sup>2+</sup>]<sub>i</sub> via VOCs in both primary mouse  $\beta$ -cells and rat islets [32, 34].

The molecular mechanism of K<sub>ATP</sub> channels closure in response to carbachol treatment is unknown. However, one possibility is that carbachol activation of PLC $\beta$  could lead to a decrease in plasma membrane PIP<sub>2</sub> levels, which is known to regulate K<sub>ATP</sub> channel activity in pancreatic  $\beta$ -cells [33–35]. mAChR stimulation clearly causes increased phosphoinositide turnover as indicated by the plasma membrane-to-cytoplasm translocation of eGFP-PH and increased accumulation of [<sup>3</sup>H]IP<sub>x</sub> in MIN6 cells. Yet, we could only detect relatively small decreases in PIP<sub>2</sub>, and it is unclear whether this would be sufficient to significantly alter K<sub>ATP</sub> channel activity. Changes in PIP levels were relatively greater, indicating that PIP<sub>2</sub> levels may be protected at the expense of PIP during mAChR stimulation in MIN6 cells. In another cell type, the human neuroblastoma SH-SY5Y, which endogenously expresses M<sub>3</sub> mAChRs, agonist addition stimulates much greater changes in PIP/PIP<sub>2</sub> levels (70–80% decreases) [25]. Nevertheless, it must be acknowledged that the methods used here are measuring global changes in PIP<sub>2</sub>, and it is possible that within the immediate vicinity of the activated mAChR, the changes in polyphosphoinositide levels may be greater. At present, there is no evidence that mAChRs and the signal transduction machinery necessary to modulate K<sub>ATP</sub> are brought together within a microenvironment such as a lipid raft, but

intriguingly the disruption of  $\beta$ -cell lipid rafts modifies Kv2.1 channel gating [42]. Therefore, it remains a possibility that changes in PIP<sub>2</sub> and/or PIP concentration affect ion channel activity, and hence the activation of ERK1/2.

SOC channel activation is dependent on IP<sub>3</sub>-mediated Ca<sup>2+</sup> release from the ER [43–45]. Therefore, mAChR activation of SOCs in MIN6 cells is also likely to be mediated by IP<sub>3</sub> receptor activation. mAChR activation has been shown to stimulate “capacitative” (ER store-depletion-driven) Ca<sup>2+</sup> entry in HIT-T15 cells and mouse pancreatic  $\beta$ -cells through the emptying of intracellular Ca<sup>2+</sup> stores [46]. Capacitative Ca<sup>2+</sup> entry has been reported to be relatively small in pancreatic  $\beta$ -cells, and, unlike other systems, it is not dependent on the energy status of the cell or PKC activation and is unaffected by protein phosphatase or tyrosine kinase inhibition [47]. However, capacitative Ca<sup>2+</sup> entry does affect membrane potential and could therefore influence the activity of the VOCs [48–50].

Our group had previously reported that GLP-1 stimulates ERK activation in MIN6 cells via Ca<sup>2+</sup> influx through L-type VOCs and that this is mediated by a Ras-independent mechanism [23]. Interestingly, carbachol-stimulated ERK activation also requires the activation of L-type VOCs and is in part independent of Ras activation. Therefore, it is likely that this Ras-independent but Ca<sup>2+</sup>-dependent ERK1/2 activation is mediated by L-type VOC signaling to ERK [23]. A proportion of carbachol-stimulated ERK1/2 activation is both Ras- and Ca<sup>2+</sup>-dependent: this could be occurring through the activation of Ca<sup>2+</sup>-dependent guanine nucleotide exchange factors (GEFs) for Ras such as Ras-GRP/Ras-GRF [51, 52].

The role of mAChR activation of ERK1/2 in pancreatic  $\beta$ -cells is currently unknown. However, the activation of ERK1/2 in  $\beta$ -cells, elicited by various nutrients and hormones, has been shown to be important in the stimulation of pancreatic  $\beta$ -cell proliferation, differentiation, survival, and gene transcription [15, 16, 53]. Intriguingly, M<sub>1</sub> and M<sub>3</sub> mAChR expression has been reported to be up-regulated and to stimulate islet cell proliferation during pancreatic regeneration [54], indicating that mAChR activation, possibly through the activation of ERK1/2, may play a positive role in  $\beta$ -cell proliferation. Moreover, in MIN6 cells, glucose-stimulated ERK1/2 activation has been shown to play an important role in enhancing insulin exocytosis, via the phosphorylation of synapsin I [18]. Therefore, it is also possible that mAChR activation of ERK plays a role in receptor-mediated potentiation of glucose-stimulated insulin secretion.

**Acknowledgments** We would like to thank Dr. Edith Gomez for critical reading of this manuscript and Dr. Gary B Willars for technical and statistical advice. This work was supported by a Diabetes UK studentship awarded to TPH (grant number 04/0002980).

**Conflict of interest** There is no conflict of interest that could be perceived as prejudicing the impartiality of the research reported.

**Open Access** This article is distributed under the terms of the Creative Commons Attribution Noncommercial License which permits any noncommercial use, distribution, and reproduction in any medium, provided the original author(s) and source are credited.

## References

- Ahren B (2000) Autonomic regulation of islet hormone secretion—implications for health and disease. *Diabetologia* 43(4): 393–410
- Gilon P, Henquin JC (2001) Mechanisms and physiological significance of the cholinergic control of pancreatic beta-cell function. *Endocr Rev* 22(5):565–604
- Gautam D, Han SJ, Hamdan FF, Jeon J, Li B, Li JH, Cui Y, Mears D, Lu H, Deng C, Heard T, Wess J (2006) A critical role for beta cell M3 muscarinic acetylcholine receptors in regulating insulin release and blood glucose homeostasis in vivo. *Cell Metab* 3(6):449–461. doi:10.1016/j.cmet.2006.04.009
- Kanat M, Norton L, Winnier D, Jenkinson C, DeFronzo RA, Abdul-Ghani MA Impaired early- but not late-phase insulin secretion in subjects with impaired fasting glucose. *Acta Diabetol*. doi:10.1007/s00592-011-0285-x
- Gromada J, Hughes TE (2006) Ringing the dinner bell for insulin: muscarinic M3 receptor activity in the control of pancreatic beta cell function. *Cell Metab* 3(6):390–392. doi:10.1016/j.cmet.2006.05.004
- Iismaa TP, Kerr EA, Wilson JR, Carpenter L, Sims N, Biden TJ (2000) Quantitative and functional characterization of muscarinic receptor subtypes in insulin-secreting cell lines and rat pancreatic islets. *Diabetes* 49(3):392–398
- Tang SH, Sharp GW (1997) Identification of muscarinic receptor subtypes in RINm5F cells by means of polymerase chain reaction, subcloning, and DNA sequencing. *Diabetes* 46(9):1419–1423
- Boschero AC, Szpak-Glasman M, Carneiro EM, Bordin S, Paul I, Rojas E, Atwater I (1995) Oxotremorine-m potentiation of glucose-induced insulin release from rat islets involves M3 muscarinic receptors. *Am J Physiol* 268 (2 Pt 1):E336–E342
- Gautam D, Han SJ, Duttaroy A, Mears D, Hamdan FF, Li JH, Cui Y, Jeon J, Wess J (2007) Role of the M3 muscarinic acetylcholine receptor in beta-cell function and glucose homeostasis. *Diabetes Obes Metab* 9(Suppl 2):158–169
- Bonner TI (1989) New subtypes of muscarinic acetylcholine receptors. *Trends Pharmacol Sci* 10(Suppl):11–15
- Kim JY, Yang MS, Oh CD, Kim KT, Ha MJ, Kang SS, Chun JS (1999) Signalling pathway leading to an activation of mitogen-activated protein kinase by stimulating M3 muscarinic receptor. *Biochem J* 337(Pt 2):275–280
- Wylie PG, Challiss RA, Blank JL (1999) Regulation of extracellular-signal regulated kinase and c-Jun N-terminal kinase by G-protein-linked muscarinic acetylcholine receptors. *Biochem J* 338(Pt 3):619–628
- Yagle K, Lu H, Guizzetti M, Moller T, Costa LG (2001) Activation of mitogen-activated protein kinase by muscarinic receptors in astroglial cells: role in DNA synthesis and effect of ethanol. *Glia* 35(2):111–120
- Barbosa HC, Bordin S, Anhe G, Persaud SJ, Bowe J, Borelli MI, Gagliardino JJ, Boschero AC (2008) Islet neogenesis-associated protein signaling in neonatal pancreatic rat islets: involvement of the cholinergic pathway. *J Endocrinol* 199(2):299–306
- Lawrence M, Shao C, Duan L, McGlynn K, Cobb MH (2008) The protein kinases ERK1/2 and their roles in pancreatic beta cells. *Acta Physiol (Oxf)* 192(1):11–17. doi:10.1111/j.1748-1716.2007.01785.x
- Costes S, Broca C, Bertrand G, Lajoix AD, Bataille D, Bockaert J, Dalle S (2006) ERK1/2 control phosphorylation and protein level of cAMP-responsive element-binding protein: a key role in glucose-mediated pancreatic beta-cell survival. *Diabetes* 55(8): 2220–2230
- Friedrichsen BN, Neubauer N, Lee YC, Gram VK, Blume N, Petersen JS, Nielsen JH, Moldrup A (2006) Stimulation of pancreatic beta-cell replication by incretins involves transcriptional induction of cyclin D1 via multiple signalling pathways. *J Endocrinol* 188(3):481–492
- Longuet C, Broca C, Costes S, Hani EH, Bataille D, Dalle S (2005) Extracellularly regulated kinases 1/2 (p44/42 mitogen-activated protein kinases) phosphorylate synapsin I and regulate insulin secretion in the MIN6 beta-cell line and islets of Langerhans. *Endocrinology* 146(2):643–654
- Gomez E, Powell ML, Bevington A, Herbert TP (2008) A decrease in cellular energy status stimulates PERK-dependent eIF2alpha phosphorylation and regulates protein synthesis in pancreatic beta-cells. *Biochem J* 410(3):485–493
- Palmer AE, Jin C, Reed JC, Tsien RY (2004) Bcl-2-mediated alterations in endoplasmic reticulum Ca<sup>2+</sup> analyzed with an improved genetically encoded fluorescent sensor. *Proc Natl Acad Sci USA* 101(50):17404–17409
- Babwah AV, Dale LB, Ferguson SS (2003) Protein kinase C isoform-specific differences in the spatial-temporal regulation and decoding of metabotropic glutamate receptor1a-stimulated second messenger responses. *J Biol Chem* 278(7):5419–5426
- Gnudi L, Frevert EU, Houseknecht KL, Erhardt P, Kahn BB (1997) Adenovirus-mediated gene transfer of dominant negative ras(asn17) in 3T3L1 adipocytes does not alter insulin-stimulated P13-kinase activity or glucose transport. *Mol Endocrinol* 11(1):67–76
- Gomez E, Pritchard C, Herbert TP (2002) cAMP-dependent protein kinase and Ca<sup>2+</sup> influx through L-type voltage-gated calcium channels mediate Raf-independent activation of extracellular regulated kinase in response to glucagon-like peptide-1 in pancreatic beta-cells. *J Biol Chem* 277(50):48146–48151
- Moore CE, Xie J, Gomez E, Herbert TP (2009) Identification of cAMP-dependent kinase as a third in vivo ribosomal protein S6 kinase in pancreatic beta-cells. *J Mol Biol* 389(3):480–494
- Willars GB, Nahorski SR, Challiss RA (1998) Differential regulation of muscarinic acetylcholine receptor-sensitive polyphosphoinositide pools and consequences for signaling in human neuroblastoma cells. *J Biol Chem* 273(9):5037–5046
- Berridge MJ, Irvine RF (1984) Inositol trisphosphate, a novel second messenger in cellular signal transduction. *Nature* 312(5992):315–321
- Lu Z, Liu D, Hornia A, Devonish W, Pagano M, Foster DA (1998) Activation of protein kinase C triggers its ubiquitination and degradation. *Mol Cell Biol* 18(2):839–845
- Wilkinson SE, Parker PJ, Nixon JS (1993) Isoenzyme specificity of bisindolylmaleimides, selective inhibitors of protein kinase C. *Biochem J* 294(Pt 2):335–337
- Martiny-Baron G, Kazanietz MG, Mischak H, Blumberg PM, Kochs G, Hug H, Marme D, Schachtele C (1993) Selective inhibition of protein kinase C isozymes by the indolocarbazole Go 6976. *J Biol Chem* 268(13):9194–9197
- Toullec D, Pianetti P, Coste H, Bellevergue P, Grand-Perret T, Ajakane M, Baudet V, Boissin P, Boursier E, Loriolle F et al (1991) The bisindolylmaleimide GF 109203X is a potent and selective inhibitor of protein kinase C. *J Biol Chem* 266(24): 15771–15781

31. Missiaen L, Callewaert G, De Smedt H, Parys JB (2001) 2-Aminoethoxydiphenyl borate affects the inositol 1, 4, 5-trisphosphate receptor, the intracellular  $\text{Ca}^{2+}$  pump and the non-specific  $\text{Ca}^{2+}$  leak from the non-mitochondrial  $\text{Ca}^{2+}$  stores in permeabilized A7r5 cells. *Cell Calcium* 29(2):111–116. doi: [10.1054/ceca.2000.0163](https://doi.org/10.1054/ceca.2000.0163)
32. Henquin JC, Garcia MC, Bozem M, Hermans MP, Nenquin M (1988) Muscarinic control of pancreatic B cell function involves sodium-dependent depolarization and calcium influx. *Endocrinology* 122(5):2134–2142
33. Shyng SL, Nichols CG (1998) Membrane phospholipid control of nucleotide sensitivity of KATP channels. *Science* 282(5391):1138–1141
34. Nakano K, Suga S, Takeo T, Ogawa Y, Suda T, Kanno T, Wakui M (2002) Intracellular  $\text{Ca}^{2+}$  modulation of ATP-sensitive  $\text{K}^{+}$  channel activity in acetylcholine-induced activation of rat pancreatic beta-cells. *Endocrinology* 143(2):569–576
35. Lin CW, Yan F, Shimamura S, Barg S, Shyng SL (2005) Membrane phosphoinositides control insulin secretion through their effects on ATP-sensitive  $\text{K}^{+}$  channel activity. *Diabetes* 54(10):2852–2858
36. Kavran JM, Klein DE, Lee A, Falasca M, Isakoff SJ, Skolnik EY, Lemmon MA (1998) Specificity and promiscuity in phosphoinositide binding by pleckstrin homology domains. *J Biol Chem* 273(46):30497–30508
37. Hirose K, Kadowaki S, Tanabe M, Takeshima H, Iino M (1999) Spatiotemporal dynamics of inositol 1, 4, 5-trisphosphate that underlies complex  $\text{Ca}^{2+}$  mobilization patterns. *Science* 284(5419):1527–1530
38. Nash MS, Young KW, Challiss RA, Nahorski SR (2001) Intracellular signalling. Receptor-specific messenger oscillations. *Nature* 413(6854):381–382. doi: [10.1038/35096643](https://doi.org/10.1038/35096643)
39. Okubo Y, Kakizawa S, Hirose K, Iino M (2001) Visualization of IP(3) dynamics reveals a novel AMPA receptor-triggered IP(3) production pathway mediated by voltage-dependent  $\text{Ca}^{2+}$  influx in Purkinje cells. *Neuron* 32(1):113–122
40. Thore S, Dyachok O, Tengholm A (2004) Oscillations of phospholipase C activity triggered by depolarization and  $\text{Ca}^{2+}$  influx in insulin-secreting cells. *J Biol Chem* 279(19):19396–19400. doi: [10.1074/jbc.C400088200](https://doi.org/10.1074/jbc.C400088200)
41. Tamarina NA, Kuznetsov A, Rhodes CJ, Bindokas VP, Philipson LH (2005) Inositol (1, 4, 5)-trisphosphate dynamics and intracellular calcium oscillations in pancreatic beta-cells. *Diabetes* 54(11):3073–3081
42. Xia F, Gao X, Kwan E, Lam PP, Chan L, Sy K, Sheu L, Wheeler MB, Gaisano HY, Tsushima RG (2004) Disruption of pancreatic beta-cell lipid rafts modifies  $\text{Kv}2.1$  channel gating and insulin exocytosis. *J Biol Chem* 279(23):24685–24691. doi: [10.1074/jbc.M314314200](https://doi.org/10.1074/jbc.M314314200)
43. Venkatachalam K, van Rossum DB, Patterson RL, Ma HT, Gill DL (2002) The cellular and molecular basis of store-operated calcium entry. *Nat Cell Biol* 4(11):E263–E272
44. Parekh AB, Penner R (1997) Store depletion and calcium influx. *Physiol Rev* 77(4):901–930
45. Putney JW Jr, Broad LM, Braun FJ, Lievreumont JP, Bird GS (2001) Mechanisms of capacitative calcium entry. *J Cell Sci* 114(Pt 12):2223–2229
46. Mears D, Zimlikli CL (2004) Muscarinic agonists activate  $\text{Ca}^{2+}$  store-operated and -independent ionic currents in insulin-secreting HIT-T15 cells and mouse pancreatic beta-cells. *J Membr Biol* 197(1):59–70. doi: [10.1007/s00232-003-0642-y](https://doi.org/10.1007/s00232-003-0642-y)
47. Liu YJ, Gylfe E (1997) Store-operated  $\text{Ca}^{2+}$  entry in insulin-releasing pancreatic beta-cells. *Cell Calcium* 22(4):277–286
48. Worley JF III, McIntyre MS, Spencer B, Mertz RJ, Roe MW, Dukes ID (1994) Endoplasmic reticulum calcium store regulates membrane potential in mouse islet beta-cells. *J Biol Chem* 269(20):14359–14362
49. Bertram R, Smolen P, Sherman A, Mears D, Atwater I, Martin F, Soria B (1995) A role for calcium release-activated current (CRAC) in cholinergic modulation of electrical activity in pancreatic beta-cells. *Biophys J* 68(6):2323–2332
50. Gilon P, Arredouani A, Gailly P, Gromada J, Henquin JC (1999) Uptake and release of  $\text{Ca}^{2+}$  by the endoplasmic reticulum contribute to the oscillations of the cytosolic  $\text{Ca}^{2+}$  concentration triggered by  $\text{Ca}^{2+}$  influx in the electrically excitable pancreatic B-cell. *J Biol Chem* 274(29):20197–20205
51. Ebinu JO, Bottorff DA, Chan EY, Stang SL, Dunn RJ, Stone JC (1998) RasGRP, a Ras guanyl nucleotide-releasing protein with calcium- and diacylglycerol-binding motifs. *Science* 280(5366):1082–1086
52. Farnsworth CL, Freshney NW, Rosen LB, Ghosh A, Greenberg ME, Feig LA (1995) Calcium activation of Ras mediated by neuronal exchange factor Ras-GRF. *Nature* 376(6540):524–527
53. Briaud I, Lingohr MK, Dickson LM, Wrede CE, Rhodes CJ (2003) Differential activation mechanisms of Erk-1/2 and p70(S6 K) by glucose in pancreatic beta-cells. *Diabetes* 52(4):974–983
54. Renuka TR, Savitha B, Paulose CS (2005) Muscarinic M1 and M3 receptor binding alterations in pancreas during pancreatic regeneration of young rats. *Endocr Res* 31(4):259–270